J. CHEM. SOC. FARADAY TRANS., 1990, 86(19), 3191–3196

Electron Paramagnetic Resonance and ENDOR Study of Semiquinones in Reversed Micelles

Dominique Niethammer, Burkhard Kirste* and Harry Kurreck*
Institut für Organische Chemie der Freien Universität Berlin, Takustr. 3, 1000 Berlin 33, Federal Republic of Germany

A series of substituted *p*-benzosemiquinone radical anions have been investigated in reversed micelles by EPR and ENDOR spectroscopies. Compared with EPR studies in homogeneous aqueous phases or in alcoholic solutions, small but significant changes in *g* values and hyperfine splittings were observed. Particularly interesting is the observation of asymmetric line-broadening effects in reversed-micellar solutions. Computer simulations of the EPR spectra demonstrate that different molecular positions make distinctly different contributions to this effect, and the ENDOR spectra exhibit a selective broadening of some of the signal pairs. It is concluded that the semiquinone anion radicals are immobilized at the surfactant–water interface. Models for the preferred location and anisotropic motion are discussed. The effect of bulky alkyl groups such as t-butyl on the spin density distribution in semiquinones in polar protic solvents is rationalized in terms of a hydrophobic effect.

Reversed micelles have recently found interest because they are capable of hosting polar water-soluble species, *e.g.* enzymatically active biomolecules, within aqueous compartments in organic solvents.[1] In contrast to normal micelles ('oil in water'), reversed micelles (also called inverse micelles) are 'water-in-oil' microemulsions consisting of an internal aqueous microphase (water pool) surrounded by a surfactant layer and the external organic phase. Reversed micelles are also an attractive medium for EPR and electron nuclear double resonance (ENDOR) studies of water-soluble radical ions. They are superior to homogeneous aqueous phases, which render EPR investigations quite difficult because the strong microwave absorption of water puts tight restrictions on the sample volume. This problem is even more severe with respect to ENDOR studies and is aggravated by the limited viscosity range available in aqueous solutions.

The feasibility of ENDOR experiments in reversed micelles was first demonstrated by Janzen *et al.* who studied Fremy's salt (sodium peroxylamine disulphonate) and detected ^{14}N ENDOR signals.[2] Bretz and co-workers extended the method to (bio-)organic radicals and obtained ENDOR spectra of lumiflavin, riboflavin, FMN and FAD radical anions in hexane–hexan-1-ol–CTAB(cetyltrimethylammonium bromide)–water reversed micelles.[3,4] In that study, a stabilization of the flavin radical anions in the reversed micelles was observed. Moreover, it is believed that spin exchange between radicals is greatly reduced because most likely only a single radical is incorporated in any one compartment. The adverse effect of dissolved oxygen on EPR linewidths is also substantially diminished in reversed-micellar solutions.[2,5]

EPR investigations of spin probes in reversed micelles can also provide a better understanding of the physicochemical properties of these systems, *i.e.* the preferred location and the mobility of the guest molecules. So far, nitroxide spin probes have been used for this purpose, and nitroxide radicals with different charge and size have been studied.[6–9] The present paper deals with an EPR and ENDOR study of a series of substituted benzosemiquinone radical anions in reversed-micellar solutions. These species were chosen because they are water soluble, fairly stable and known to give strong proton ENDOR signals;[10,11] for a review of EPR spectroscopy of semiquinones, see the article by Pedersen.[12] The ENDOR technique was applied not only as an aid in unravelling hyperfine patterns but also because it easily enables unambiguous detection of specific line broadening of individual proton hyperfine components. Important information about the anchoring of the semiquinone radical anions at the water–surfactant interface could be obtained.

Experimental

Preparation of Quinones

All quinones investigated in this study have been described in the literature; some of them are commercially available. However, our method of oxidation of the respective hydroquinones has not, to our knowledge, been described previously. 2-Methyl-1,4-benzoquinone (**2**), 2,3-dimethyl-1,4-benzoquinone (**3**) and 2-t-butyl-1,4-benzoquinone (**4**) were obtained by oxidation of the alkylhydroquinones in acetone–water (1 : 1) or acetic acid–water (1 : 1) with ammonium peroxodisulphate, and recrystallized from n-pentane (yields 90–98%). 2-Cyclohexyl-1,4-benzoquinone (**5**) and 2,5-dicyclohexyl-1,4-benzoquinone (**6**)[13] were prepared by alkylation of 1,4-benzoquinone (**1**) according to the method of Jacobsen and Torssell[14] *via* oxidative decarboxylation of cyclohexanecarboxylic acid.

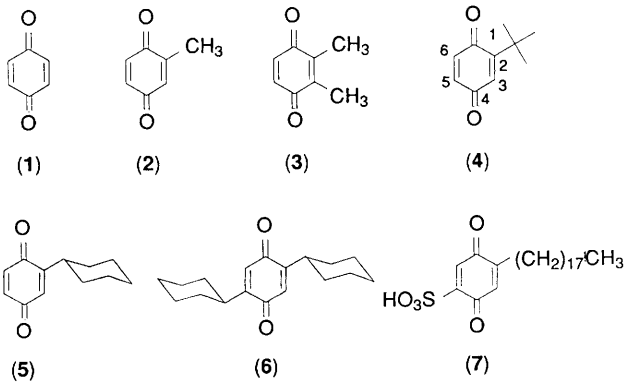

Scheme 1

2-Cyclohexyl-1,4-benzoquinone (**5**)

1,4-Benzoquinone (50 mmol), cyclohexanecarboxylic acid (60 mmol) and $AgNO_3$ (6 mmol) were dissolved in a mixture of water (100 cm^3) and CH_2Cl_2 (100 cm^3). This mixture was stirred at 45 °C, and a solution of $(NH_4)_2S_2O_8$ (60 mmol) in water (100 cm^3) was added dropwise for 90 min. After gas evolution had stopped, the organic phase was separated,

dried over Na_2SO_4, and the solvent was removed. The residue was extracted with n-pentane and the product was recrystallized from ethanol: 53% yield; m.p. 53–54 °C (55 °C[13]); $m/z = 190$ (M^+); NMR ($CDCl_3$) $\delta = 1.2$ ppm (3H, m), $\delta = 1.41$ ppm (2H, m, eq), $\delta = 1.84$ ppm (5H, m), $\delta = 2.70$ ppm (1H, ttd, $^3J_{aa} = 11.7$ Hz, $^3J_{ae} = 2.9$ Hz, $^4J = 1.1$ Hz, ax), $\delta = 6.52$ ppm (1H, dd, $^4J_{35} = 2.2$ Hz, $^4J_{32\beta} = 1.1$ Hz, H-3), $\delta = 6.70$ ppm (1H, dd, $^3J_{56} = 10$ Hz, $^4J_{35} = 2.2$ Hz, H-5), $\delta = 6.75$ (1H, d, $^3J_{56} = 10$ Hz, H-6).

2,5-*Dicyclohexyl*-1,4-*benzoquinone* (**6**)

This was prepared similarly from 1,4-benzoquinone (0.1 mol), cyclohexanecarboxylic acid (0.3 mol), $(NH_4)_2S_2O_8$ (0.35 mol) and $AgNO_3$ (0.035 mol). After extraction and recrystallization, a mixture of 2,5- (**6**) and 2,6-dicyclohexyl-1,4-benzoquinone and **5** was obtained which was separated by column chromatography ($CHCl_3/SiO_2$): 14% yield; m.p. 138 °C (138 °C[13]); $m/z = 272$ (M^+); NMR ($CDCl_3$) $\delta = 1.22$ ppm (6H, m), $\delta = 1.41$ ppm (4H, m), $\delta = 1.79$ ppm (10H, m), $\delta = 2.68$ ppm (2H, tt), $\delta = 6.48$ ppm (2H, s).

Sample Preparation

Reversed micelles were prepared with either n-heptane–chloroform (1 : 1) or cyclohexane–2-methylhexan-2-ol (5 : 1) as organic solvent. Cetyltrimethylammonium bromide (CTAB) was used as cationic surfactant in concentrations of 0.2–0.3 mol dm^{-3}. Stock solutions were stored under argon. Aqueous solution (usually 1 mol dm^{-3} KOH, 1 mol dm^{-3} KBr) was added in the proper amount to give the desired W_0 value of 10–15; W_0 is defined as the ratio of molar concentrations [water]/[surfactant]. The formation of reversed micelles was accelerated by ultrasonification. The respective quinone was added as solid, and the remaining oxygen was removed by flushing the solution briefly with argon. Semiquinone radical anions formed spontaneously in the alkaline solutions, hence addition of a reductant was not necessary. For EPR/ENDOR measurements, cylindrical pyrex sample tubes with 3.5 mm o.d. (*ca.* 3.0 mm i.d.) were used. Homogeneous alkaline aqueous solutions of the semiquinones were prepared by dissolving the quinones in 0.1 mol dm^{-3} LiOH; capillary tubes were used for EPR measurements. Solutions of the semiquinones in 2-propanol were generated from the quinones with a trace of benzoin as reductant and benzyltrimethylammonium hydroxide as base.

Instrumentation

EPR and ENDOR spectra were recorded on a Bruker ER 220D EPR spectrometer equipped with a Bruker cavity (ER200ENB) and laboratory-built NMR facilities described elsewhere.[15,16] The temperature of the sample was adjusted by means of a Bruker VT-1000 temperature control unit. The spectrometer was interfaced with a minicomputer (HP1000/A600) used for data acquisition in ENDOR experiments and handling and storage of the spectra. EPR spectra were accumulated by using a Nicolet 1170 signal-averager employing 1024 data points and afterwards transferred to the minicomputer. Alternatively, a Bruker ER 200D-SRC EPR spectrometer was used which was interfaced with a Comtec AT286/10 microcomputer *via* a MetraByte DAS-16 board. The microwave frequency was measured with an HP5245L/5255A frequency counter and the magnetic field strength ($B_0 \approx 0.34$ T) with a Bruker ER035M NMR gaussmeter. In *g*-factor measurements, field gradients were corrected for by replacing the sample with a reference compound (phenalenyl in toluene, $g = 2.002\,62$). Spectrum simulations were performed on one of the above-mentioned computers or on an IBM-RT 6150-125 by means of the programs EPRFT or HFFIT (see below).

Results

In fig. 1, the EPR spectra of $\mathbf{4}^{\bullet -}$ recorded in alkaline aqueous solution (*a*) are compared with those obtained in reversed-micellar solution (*b*), (*c*). The eight-line hyperfine pattern is due to the interaction with three inequivalent ring protons, the t-butyl protons merely give rise to some inhomogeneous line broadening. The EPR spectra recorded in reversed-micellar solution differ from those obtained in homogeneous aqueous (or alcoholic) solution in four respects. First, the *g* value increases from 2.004 64 (0.1 mol dm^{-3} LiOH, 300 K) to 2.004 80 (reversed micelle, $W_0 = 10$, 300 K). Secondly, the hyperfine coupling constants, especially the largest one, are altered (see table 1). Thirdly, the linewidths are increased and fourthly, most dramatically, a pronounced asymmetric line-broadening effect is observed. As might have been expected, the linewidth effects are more severe at lower temperatures. An increase in linewidths was also observed with increasing W_0-values ($W_0 = 10$–15). On the other hand, the counterion (lithium, sodium, potassium or benzyltrimethylammonium) has no noticeable influence on hyperfine splittings or linewidths. The reversed-micellar solutions of the semiquinones could be stored in a freezer for weeks without noticeable decomposition, but the radicals decompose gradually on heating above 320 K. At room temperature, the radicals are more stable in these samples than in propan-2-ol.

For isotropic fluid solution ENDOR studies propan-2-ol was used as solvent [fig. 1(*d*)]. This secondary alcohol proved superior over methanol or ethanol because the semiquinones are known to react with primary alcohols rather rapidly.[17] Our attempts to record ENDOR spectra in aqueous solution have failed so far. (The feasibility of performing ENDOR in liquid water was previously demonstrated, using a crown ether substituted naphthosemiquinone radical anion.[18])

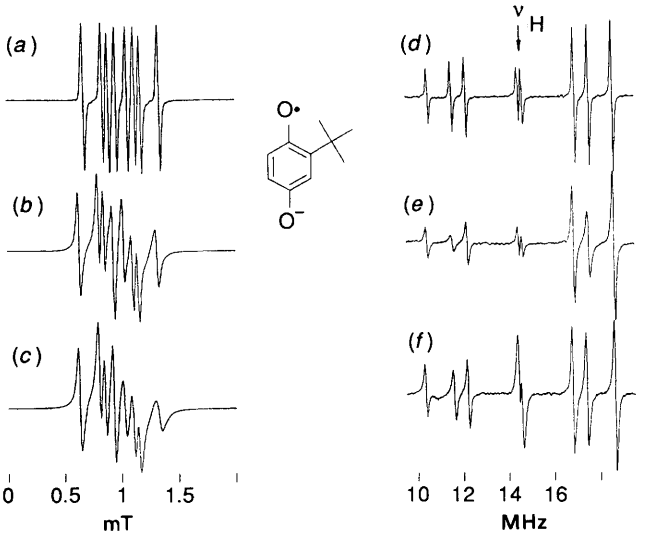

Fig. 1. EPR and ENDOR spectra of $\mathbf{4}^{\bullet -}$. EPR (*a*) in water, 0.1 mol dm^{-3} LiOH, 300 K, (*b*) in reversed-micellar solution, 0.3 mol dm^{-3} CTAB, $CHCl_3$–n-heptane (1 : 1), 1 mol dm^{-3} LiOH, $W_0 = 15$, 305 K and (*c*) 270 K. ENDOR (*d*) in propan-2-ol at 270 K, (*e*) in reversed-micellar solution at 290 K and (*f*) at 330 K; experimental conditions: r.f. power 130 W corresponding to $B_{RF} \approx 0.5$ mT in the rotating frame, microwave power 10 mW, modulation amplitude (FM at 10 kHz) 50 kHz; 150 scans were accumulated, scan time 40 s, time constant 40 ms. ENDOR linewidths in (*e*): 110 kHz at 16.83 MHz, 150 kHz at 17.48 MHz and 120 kHz at 18.59 MHz (not corrected for modulation and saturation broadening).

Table 1. Hyperfine coupling constants (/mT)[a] and g values of substituted 1,4-benzosemiquinone anion radicals in homogeneous and reversed-micellar solutions

	solvent	T/K	a_2	a_3	a_5	a_6	g ($\pm 10^{-5}$)
1	EtOH	200	−0.238	−0.238	−0.238	−0.238	
1	aq. LiOH[b]	300	−0.236	−0.236	−0.236	−0.236	2.004 63
1	inv. micelle[b]	300	−0.236	−0.236	−0.239	−0.236	2.004 79
2	Pr^{i}OH	260	+0.198[c]	−0.182	−0.256	−0.244	
2	aq. LiOH[b]	300	+0.210[c]	−0.172	−0.258	−0.240	2.004 55
2	inv. micelle	290	+0.209[c]	−0.174	−0.252	−0.252	2.004 65
3	Pr^{i}OH	290	+0.171[c]	+0.171[c]	−0.260	−0.260	
3	inv. micelle	300	+0.172[c]	+0.172[c]	−0.262	−0.262	
4	Pr^{i}OH	270	+0.006[d]	−0.170	−0.214	−0.288	
4	aq. LiOH[b]	300	+0.006[d]	−0.163	−0.214	−0.280	2.004 64
4	inv. micelle	290	+0.006[d]	−0.166	−0.213	−0.292	2.004 80
5	Pr^{i}OH	300	+0.113[e]	−0.179	−0.246	−0.254	
5	aq. NaOH[f]		+0.117[c]	−0.160	−0.250	−0.250	
5	inv. micelle	300	+0.134[c]	−0.167	−0.235	−0.267	
6	Pr^{i}OH	300	+0.119[g]	−0.194	+0.119[g]	−0.194	
6	inv. micelle	330	+0.127[c]	−0.195	+0.127[c]	−0.195	
7	Pr^{i}OH	290	+0.107[h]	−0.217	—	−0.293	
7	inv. micelle	290	+0.133[c]	−0.187	—	−0.334	

[a] Measured by ENDOR unless stated otherwise ($\pm 5 \times 10^{-4}$ mT; 1 mT = 28.06 MHz). Signs were determined by general TRIPLE resonance. [b] Measured by EPR; data were extracted by least-squares fitting. [c] β-protons. [d] γ-protons. [e] β-protons; further coupling constants (/mT): −0.013 (2H, γ), +0.013 (2H, δ_e), −0.005 (2H, γ). [f] EPR radical generated by irradiation of 2-cyclohexyl-4-chlorophenol in aqueous alkaline solution (pH 8).[32] [g] β-protons; further coupling constants (/mT): −0.014 (4H, γ), +0.014 (4H, δ_e), −0.006 (4H, γ). [h] β-protons; γ protons: 0.003 mT.

However, ENDOR spectra could easily be obtained from reversed-micellar solutions, see fig. 1 (*e*) and (*f*). The ENDOR spectra exhibit four pairs of lines due to the ring and t-butyl protons; the hyperfine coupling constants are collected in table 1. The ENDOR spectra obtained from reversed-micellar solutions show a remarkable line broadening and corresponding decrease in intensity of the signals due to the second largest splitting. This effect becomes more pronounced with decreasing temperature.

The EPR spectrum of $\mathbf{5}^{\bullet -}$ in propan-2-ol is depicted in fig. 2(*a*). Digital resolution enhancement by Lorentzian-to-Gaussian transformation[19] reveals further splittings [fig. 2(*b*)], *i.e.* the signals in the wings exhibit a quintet pattern which can be verified by computer simulations [fig. 2(*c*)]. In reversed-micellar solution, the signals are broadened and an asymmetric linewidth effect is observed, although it is less obvious than in the case of $\mathbf{4}^{\bullet -}$, see fig. 2(*d*). The ENDOR spectra of $\mathbf{5}^{\bullet -}$ in propan-2-ol and in the reversed-micellar solution are shown in fig. 3(*a*) and (*b*). Again, the line pair belonging to the second largest splitting is selectively broadened. Relative signs of the hyperfine coupling constants were determined by general (electron–nuclear–nuclear) TRIPLE resonance.[16,20] The largest three couplings have the same sign. They can be assigned to the ring protons, and their absolute sign may safely be assumed to be negative. The fourth coupling is positive and may be assigned to the β proton, *i.e.* position 1 of the cyclohexyl moiety. The fifth coupling does not exhibit a general TRIPLE effect, *i.e.* protons with couplings of

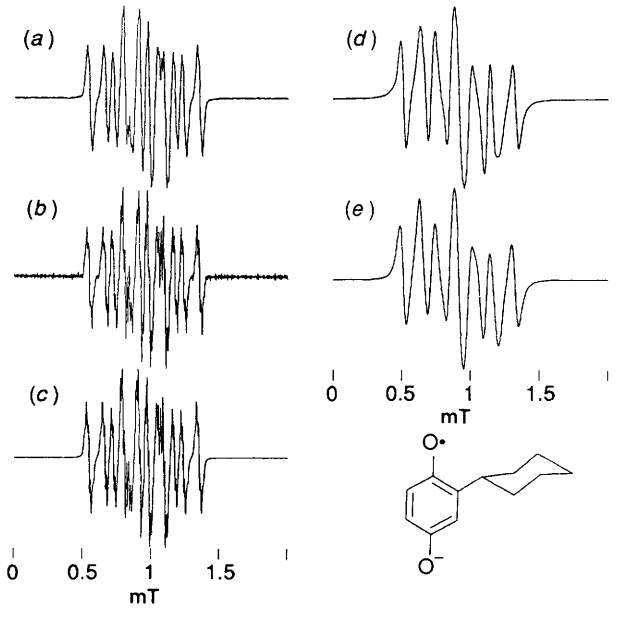

Fig. 2. EPR spectra of $\mathbf{5}^{\bullet -}$ (*a*) in propan-2-ol at 310 K and (*d*) in reversed-micellar solution, 0.2 mol dm^{-3} CTAB, 2-methylhexan-2-ol/cyclohexane (1 : 5), 1 mol dm^{-3} KOH, 1 mol dm^{-3} KBr, W_0 = 10, 300 K. Spectrum (*b*) was obtained by digital resolution enhancement (Lorentzian-to-Gaussian transformation, LB = −0.01 mT, GB = 0.3); (*c*) and (*e*) are computer-simulated spectra.

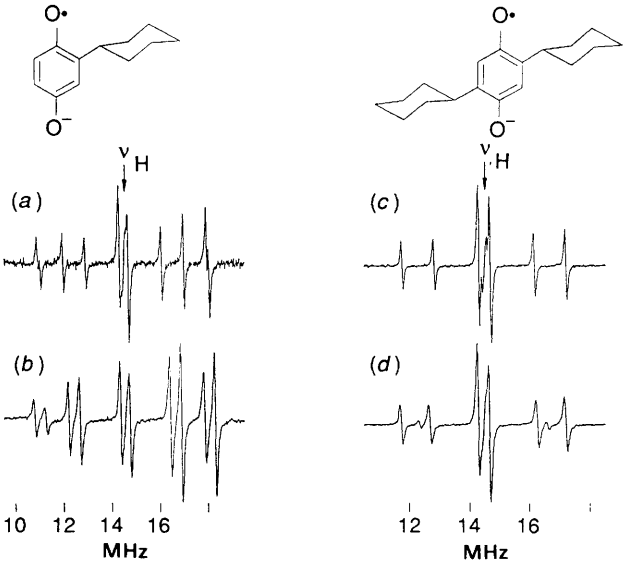

Fig. 3. ENDOR spectra of (*a*) $\mathbf{5}^{\bullet -}$ in propan-2-ol at 300 K, (*b*) $\mathbf{5}^{\bullet -}$ in reversed-micellar solution [*cf.* fig. 2(*b*)] at 300 K, (*c*) $\mathbf{6}^{\bullet -}$ in propan-2-ol at 300 K and (*d*) $\mathbf{6}^{\bullet -}$ in reversed-micellar solution at 330 K, W_0 = 15.

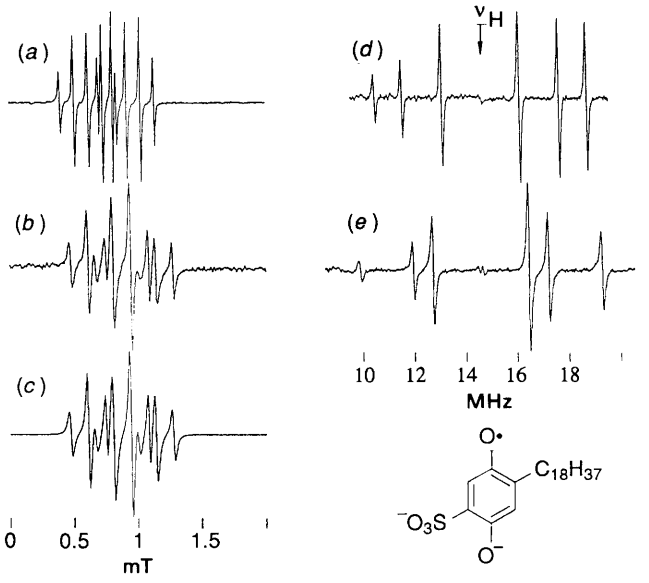

Fig. 4. EPR and ENDOR spectra of $\mathbf{7}^{\bullet -}$. EPR: (*a*) in propan-2-ol at 290 K; (*b*) in reversed-micellar solution, 0.2 mol dm^{-3} CTAB, 2-methylhexan-2-ol–cyclohexane (1 : 5), 1 mol dm^{-3} KOH, 1 mol dm^{-3} KBr, $W_0 = 20$, 290 K; (*c*) computer simulation. ENDOR (*d*) in propan-2-ol at 290 K and (*e*) in reversed-micellar solution at 290 K.

opposite signs contribute equally, whereas the smallest coupling (0.005 mT) is negative. [For a discussion of spin density transfer into cyclohexyl groups see ref. (21).]

Radical generation of the disubstituted semiquinone $\mathbf{6}^{\bullet -}$ in reversed micelles proved to be substantially more difficult than with the monosubstituted compound. The ENDOR spectra of $\mathbf{6}^{\bullet -}$ in propan-2-ol and in a reversed micelle are compared in fig. 3(*c*) and (*d*). The spectrum recorded in the reversed-micellar solution reveals the presence of a small amount of decomposition product, but the hyperfine couplings of $\mathbf{6}^{\bullet -}$ are almost unaltered in the two solvents (see table 1).

The 2-methylsemiquinone radical anion $\mathbf{2}^{\bullet -}$ has also been investigated in homogeneous solution (EPR in water, ENDOR in propan-2-ol) and in reversed micelles (EPR, ENDOR). The data are collected in table 1. In the reversed-micellar solution the two ring protons with the largest hyperfine coupling have the same value, hence detailed information on specific line broadening is not available. In the disubstituted semiquinone $\mathbf{3}^{\bullet -}$, there is again little difference in the hyperfine couplings when comparing homogeneous and reversed-micellar solutions (see table 1). Finally, the 'amphiphilic' semiquinone $\mathbf{7}^{\bullet -}$ will be considered. EPR and ENDOR spectra recorded in homogeneous and in reversed-micellar solutions are depicted in fig. 4. The hyperfine couplings measured in the latter deviate considerably from those obtained in propan-2-ol (see table 1).

Discussion

For the rationalization of the asymmetric linewidth effect observed in the EPR spectra of semiquinones in the reversed-micellar solutions, a simplified approach was taken. Whereas nitroxide spin probes are essentially characterized by a single hyperfine coupling, *i.e.* the nitrogen coupling, several proton coupling constants must be taken into account in the case of the semiquinones. In the fast-tumbling (Redfield) regime, the asymmetric linewidth effect of nitroxide radicals can be described adequately by the following M_I dependence:[22]

$$T_2^{-1} = A + BM_I + CM_I^2 \qquad (1)$$

where B depends on the inner product of the $\boldsymbol{g}$ tensor and the dipolar hyperfine tensor $\boldsymbol{A}'$ ($\boldsymbol{g}' : \boldsymbol{A}'$) and C on ($\boldsymbol{A}' : \boldsymbol{A}'$); A depends on both ($\boldsymbol{g}' : \boldsymbol{g}'$) and ($\boldsymbol{A}' : \boldsymbol{A}'$) but is also influenced by field inhomogeneities, unresolved hyperfine splittings, exchange effects *etc.* and is usually less useful for linewidth analyses. Eqn (1) can be extended to the more general case of an electron spin interacting with several non-equivalent nuclei, but in this case cross-terms of the type $E_{ij}M_{Ii}M_{Ij}$ depending on ($\boldsymbol{A}_i' : \boldsymbol{A}_j'$) also have to be taken into account, see eqn (2):[23,24]

$$T_2^{-1} = A + \sum_i B_i M_{Ii} + \sum_i C_i M_{Ii}^2 + \sum_{\substack{i,j \\ i<j}} E_{ij} M_{Ii} M_{Ij}. \qquad (2)$$

We were primarily interested in finding out whether the EPR spectra would provide direct evidence on which protons were mainly responsible for the observed asymmetric linewidth effect. In particular, we wanted to check to what extent the specific line broadening observed in some of the ENDOR spectra would find a correspondence in the EPR spectra. In a first series of simulations, we therefore neglected the cross-terms E_{ij} in eqn (2). Moreover, the C terms were not explicitly taken into account in the case of single non-equivalent protons ($M_I = \pm\frac{1}{2}$) because their effect is experimentally indistinguishable from that of the A term. However, the neglect of the cross-terms is not really justified since theoretical estimates indicate that the inner products ($\boldsymbol{A}_i' : \boldsymbol{A}_j'$) are comparable to $\mu_B B_0(\boldsymbol{g}' : \boldsymbol{A}_i')$. Therefore, we performed a second series of simulations (only for the EPR spectra of $\mathbf{4}^{\bullet -}$) in which we tried to optimize the linewidths individually. In this case, the coefficients of eqn (2) were evaluated afterwards by multilinear regression analysis.

For simulations and iterative least-squares fitting, the program HFFIT described previously[25] (rewritten to the C language) was modified either to handle M_I-dependent linewidths in the simplified manner described above or to optimize the widths of all hyperfine lines independently. Using the restricted model (neglecting cross-terms), the agreement with the experimental spectra is satisfactory, but not surprisingly, a significantly better match has been achieved when all linewidths were allowed to vary freely. Some results obtained for $\mathbf{4}^{\bullet -}$ by means of the latter method are depicted in fig. 5. The resulting B parameters [see eqn (2)] are collected in table 2. It can be seen that the second largest hyperfine coupling is in fact mostly responsible for the asymmetric

Table 2. EPR linewidth coefficients ($/\mu$T) of 2-substituted 1,4-benzosemiquinone anion radicals in reversed-micellar solution[a]

	W_0	T/K	A	B_3	B_5	B_6	E_{35}	E_{36}	E_{56}
4	15	280	39.5[b]	5.5	9.3	6.9	6.6	7.0	12.4
4	15	290	43.7[b]	5.1	8.4	6.2	6.1	7.3	12.8
4	15	305	35.8[b]	2.8	4.5	3.1	0.4	5.4	8.8
4	15	310	32.4[b]	2.4	3.1	1.8	−0.4	4.1	6.2
4	10	280	30.7[b]	3.6	5.2	3.2	5.2	4.1	5.8
4	10	290	27.0[b]	2.3	3.1	2.1	4.0	2.6	3.8
4	10	300	25.6[b]	1.6	2.3	1.5	3.2	1.9	3.1

	W_0	T/K	A	B_2	C_2	B_3	B_5	B_6
2	15	310	13.9	0.3	−0.1	0.7	1.7[c]	0.1[c]
5	10	300	38.7[b]	1.5	—	1.0	3.3	1.2
7	20	290	23.6	2.6	0.8	4.3	—	−0.8

[a] Results of least-squares fitting using the linewidth model of eqn (2); cross-terms E_{ij} were only taken into account in the case of compound **4**, see text. The coefficients refer to peak-to-peak linewidths, first-derivative Lorentzian lineshape is assumed. Assignments correspond to those used in table 1. [b] Including inhomogeneous broadening due to unresolved hyperfine splittings. [c] Positions 5 and 6 cannot be distinguished since $a_5 = a_6$.

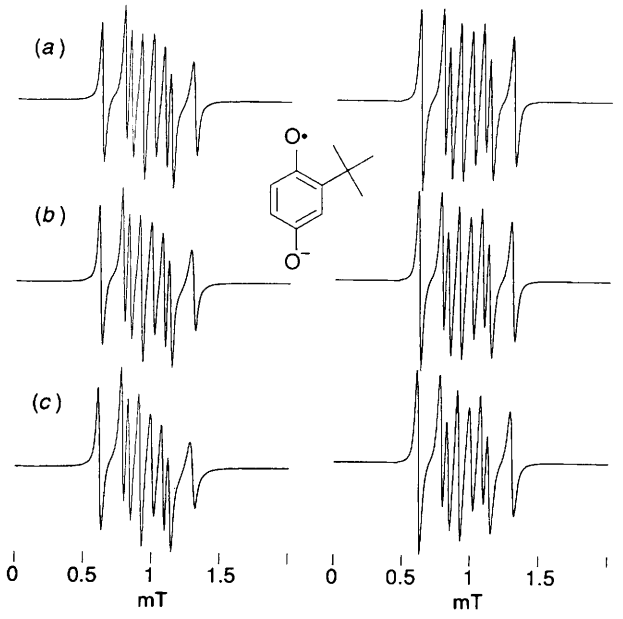

Fig. 5. EPR spectra of $\mathbf{4}^{\bullet -}$ in reversed-micellar solution, 0.3 mol dm^{-3} CTAB, $CHCl_3$–n-heptane (1 : 1), 1 mol dm^{-3} LiOH, $W_0 = 10$, at different temperatures: (*a*) 300, (*b*) 290, (*c*) 280 K. In each case, the left trace is the experimental spectrum; the right trace is the computer-simulated spectrum.

linewidth effect, in accordance with the specific line broadening in the ENDOR spectra. However, the effect of the other protons is not completely negligible.

The *B* parameters increase with decreasing temperature or with increasing values of W_0. Thus, the mobility of the semiquinone radical anions decreases with decreasing temperature. Since the linewidths are much larger than in homogeneous aqueous solution (see fig. 1), the semiquinones must be immobilized somehow by being anchored at the surfactant–water interface. A decreasing mobility with increasing W_0, *i.e.* increasing size of reversed micelles, was also observed in a previous study dealing with nitroxide radicals.[8] This behaviour can easily be rationalized by considering the slower tumbling of the reversed micelles as a whole with increasing size of the water compartments. Note that the total mobility of the radicals, which is responsible for the relaxation effects, may be seen as a combination of the motion of the radicals within the reversed micelle and of the motion of the compartment as a whole.

Interesting points to be discussed are the position of anchoring and its consequences for the linewidth effects and the observed changes of *g* values and hyperfine couplings when comparing homogeneous aqueous solutions with reversed-micellar systems. First, it should be noted that substantial changes in these parameters are only observed with semiquinones, which are unsymmetrically substituted with respect to the oxygen atoms ($\mathbf{2}^{\bullet -}$, $\mathbf{4}^{\bullet -}$, $\mathbf{5}^{\bullet -}$, $\mathbf{7}^{\bullet -}$). Hence, it may be concluded that an unsymmetrical solvation must play an important role. Since in none of the symmetrical radicals ($\mathbf{3}^{\bullet -}$, $\mathbf{6}^{\bullet -}$) including the parent 1,4-benzosemiquinone ($\mathbf{1}^{\bullet -}$) is an additional splitting, *i.e.* loss of symmetry, observed in reversed micelles, it may be concluded that a flipping between different but equivalent anchoring sites is rapid on the EPR timescale.

For a further discussion it is clearly necessary to know the assignment of the hyperfine coupling constants to molecular positions. Owing to the lack of availability of specifically deuteriated quinones one must rely on calculations.[26] The hyperfine couplings of $\mathbf{2}^{\bullet -}$ have been assigned by means of Hückel Molecular Orbital–McLachlan calculations.[27] In another study, the same sequence was assumed to apply to $\mathbf{4}^{\bullet -}$, *i.e.* the largest splitting was assigned to position 5, the second largest to position 6, and the smallest to position 3.[28] However, on the basis of this assignment we did not see a reasonable explanation for the specific line-broadening effect observed in reversed micelles; why should it be position 6 which is predominantly affected?

When comparing hyperfine data for $\mathbf{2}^{\bullet -}$ and $\mathbf{4}^{\bullet -}$, one finds significant differences, see table 1. One may attempt an explanation by assuming a larger inductive effect of the t-butyl group than of the methyl group.[28] However, it is clear that environment effects must be taken into account. A particularly striking example is offered by the 2,6-di-t-butyl-1,4-benzosemiquinone radical anion: the ring proton coupling is 0.131 mT in water but 0.225 mT in HMPA.[29] (We have measured 0.108 mT in the reversed-micellar solution, $W_0 = 15$, 300 K.) Obviously, solvent properties such as hydrogen bonding are responsible for this effect. Although the Hückel Molecular Orbital–McLachlan method is not very sophisticated, it can accommodate solvent effects by using altered heteroatom parameters. Thus, the effect of hydrogen bonding will be an increase of the effective electronegativity at the oxygen atoms, which can be expressed by an increased value of the Coulomb parameter, h_o. In fact, a reasonable explanation of the solvent dependence of hyperfine coupling constants and *g* values in unsubstituted and methyl-substituted *p*-benzosemiquinone radical anions could be given that way (DMSO: $h_o = 1.46$, $k_{OC} = 1.298$; H_2O: $h_o = 1.72$, $k_{OC} = 1.22$).[27] In polar protic solvents capable of forming hydrogen bonds, *g* values smaller than in aprotic solvents are observed ($\mathbf{1}^{\bullet -}$ in H_2O: $g = 2.004\,69$; in DMSO: $g = 2.005\,41$[27]). This effect may be rationalized by considering that a high spin density but not a high charge density at heteroatoms will increase the *g* value.

Now our rationale is that t-butyl groups will have a similar influence on the neighbouring oxygen atom as does a hydrocarbon solvent, and the formation of hydrogen bonds is probably prevented when the oxygen atom is surrounded by two t-butyl groups. Thus, we used the above-mentioned heteroatom parameters[27] with modifications for neighbouring t-butyl groups. As a check, we performed calculations on 2,6-di-t-butyl-1,4-benzosemiquinone with the parameters $Q^{H}_{CH} = -2.7$ mT, $k_{OC} = 1.22$ (always), $h_{o1} = 1.46$ (always), $h_{o4} = 1.46$ (HMPA) or 1.72 (H_2O) and the hyperconjugative model for the t-butyl groups with parameters suggested for methyl groups ($h_{2a} = -0.1$, $h_{2b} = -0.5$, $k_{2a} = 0.7$, $k_{2a2b} = 2.5$)[30] and obtained $a_{3,5} = 0.154$ mT (H_2O) or 0.214 mT (HMPA), respectively, in reasonable agreement with the experimental data (0.131, 0.225 mT).

Assuming that even one t-butyl group affects hydrogen bonding of the neighbouring oxygen, a calculation for $\mathbf{4}^{\bullet -}$ in water with $h_{o1} = 1.59$ yields $a_3 = 0.167$, $a_5 = 0.225$ and $a_6 = 0.250$ mT, *i.e.* the order with respect to H-5 and H-6 is reversed. This means that H-5 is mainly responsible for the line broadening effects observed in the EPR and ENDOR spectra. A qualitative explanation can then be given by assuming that $\mathbf{4}^{\bullet -}$ is anchored with the t-butyl group at the water–surfactant interface. Thus, rotations about the C_2—C_5 axis should remain essentially unaffected, whereas motions of this axis should be hindered (see fig. 6). Since H-5 lies exactly on this axis, only anisotropies perpendicular to the C_5—H bond will be averaged out rapidly, whereas components along the bond direction are subject to slow-motion effects. According to the theory of McConnell and Strathdee, the largest component of the dipolar hyperfine tensor is just along the C—H bond axis.[31] Hence, it is reasonable that H-5 is in fact predominantly affected by the anchoring of $\mathbf{4}^{\bullet -}$ at the interface. The altered *g* value may be rationalized by con-

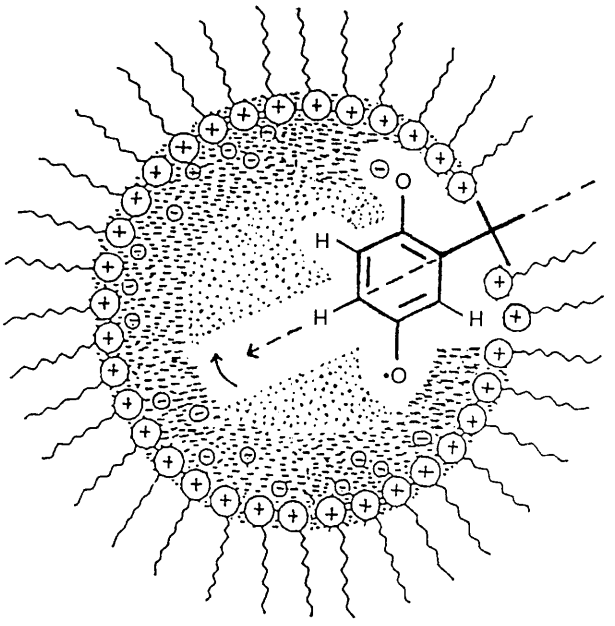

Fig. 6. Schematic representation of a reversed micelle (water inside, organic solvent outside, cationic surfactant molecules at the interface). The anchoring and principal axis of motion of a semiquinone molecule $4^{\bullet -}$ are indicated (not drawn to scale).

sidering the more hydrophobic environment of the oxygen atom which is situated close to the interface. The behaviour of the respective cyclohexyl-substituted semiquinone $5^{\bullet -}$ is analogous.

The 'amphiphilic' semiquinone $7^{\bullet -}$ is certainly anchored with the alkyl chain in the hydrophobic part of the interface, the sulphonate group being located at the aqueous side. In this case there is no C—H bond along the axis of fixation. However, simulations of the EPR spectra suggest that the β-methylene protons of the alkyl chain give a major contribution to the line-broadening effects [see fig. 4(*c*) and table 2].

Further studies with differently substituted quinones and attempts for a more quantitative analysis of the observed effects are in progress.

We thank Mrs E. Brinkhaus for her assistance in recording the EPR spectra and Dr H. Hungerbühler for supplying us with a sample of **7**. B.K. and H.K. gratefully acknowledge financial support by the Fonds der Chemischen Industrie and the Deutsche Forschungsgemeinschaft (Normalverfahren).

References

1 P. L. Luisi, *Angew. Chem.*, 1985, **97**, 449; *Angew. Chem., Int. Ed. Engl.*, 1985, **24**, 439.
2 E. G. Janzen, Y. Kotake, G. A. Coulter and U. M. Oehler, *Chem. Phys. Lett.*, 1986, **126**, 205.
3 N. Bretz, I. Mastalsky, M. Elsner and H. Kurreck, *Angew. Chem.*, 1987, **99**, 357; *Angew. Chem., Int. Ed. Engl.*, 1987, **26**, 345.
4 H. Kurreck, N. H. Bretz, N. Helle, N. Henzel and E. Weilbacher, *J. Chem. Soc., Faraday Trans. 1*, 1988, **84**, 3293.
5. M. Okazaki and K. Toriyama, *J. Magn. Reson.*, 1988, **79**, 158.
6 Y. Y. Lim and J. H. Fendler, *J. Am. Chem. Soc.*, 1978, **100**, 7490.
7 A. Barelli and H-F. Eicke, *Langmuir*, 1986, **2**, 780.
8 G. Häring, P. L. Luisi and H. Hauser, *J. Phys. Chem.*, 1988. **92**, 3574.
9 Y. Kotake and E. G. Janzen, *J. Phys. Chem.*, 1988, **92**, 6357.
10 J. S. Hyde, *J. Chem. Phys.*, 1965, **43**, 1806.
11 M. R. Das, H. D. Connor, D. S. Leniart and J. H. Freed, *J. Am. Chem. Soc.*, 1970, **92**, 2258.
12 J. A. Pedersen, *EPR Spectra from Natural and Synthetic Quinones and Quinols* (CRC Press, Boca Raton, Florida, 1985).
13 W. Flaig, T. Ploetz and H. Biergans, *Justus Liebigs Ann. Chem.*, 1956, **597**, 196.
14 N. Jacobsen and K. Torssell, *Justus Liebigs Ann. Chem.*, 1972, **763**, 135.
15 H. Kurreck, B. Kirste and W. Lubitz, *Angew. Chem.*, 1984, **96**, 171; *Angew. Chem., Int. Ed. Engl.*, 1984, **23**, 173.
16 H. Kurreck, B. Kirste and W. Lubitz, *Electron Nuclear Double Resonance Spectroscopy of Radicals in Solution* (VCH Publishers, New York, 1988).
17 N. M. Atherton and A. J. Blackhurst, *J. Chem. Soc., Faraday Trans. 2*, 1972, **68**, 470.
18 H. Bock and B. Hierholzer, *Angew. Chem.*, 1988, **100**, 1127; *Angew. Chem., Int. Ed. Engl.*, 1988, **27**, 1069.
19 K. Roth and B. Kirste, *J. Magn. Reson.*, 1985, **63**, 360.
20 R. Biehl, M. Plato and K. Möbius, *J. Chem. Phys.*, 1975, **63**, 3515.
21 B. Kirste, W. Broser, K. Grein, H. Kurreck and G. Schlömp, *Chem. Ber.*, 1985, **118**, 3464.
22 P. L. Nordio, *Spin Labeling. Theory and Applications*, ed. L. J. Berliner (Academic Press, New York, 1976), vol. 1, p. 5.
23 J. H. Freed and G. K. Fraenkel, *J. Chem. Phys.*, 1963, **39**, 326.
24 A. Hudson and G. R. Luckhurst, *Chem. Rev.*, 1969, **69**, 191.
25 B. Kirste, *J. Magn. Reson.*, 1987, **73**, 213.
26. J. A. Pedersen, *J. Chem. Soc., Perkin Trans. 2*, 1973, 424.
27 P. D. Sullivan, J. R. Bolton and W. E. Geiger Jr, *J. Am. Chem. Soc.*, 1970, **92**, 4176.
28 C. Trapp, C. A. Tyson and G. Giacometti, *J. Am. Chem. Soc.*, 1968, **90**, 1394.
29 D. M. Holton and D. Murphy, *J. Chem. Soc., Faraday Trans. 1*, 1982, **78**, 1223.
30 D. Lazdins and M. Karplus, *J. Am. Chem. Soc.*, 1965, **87**, 920.
31 H. M. McConnell and J. Strathdee, *Mol. Phys.*, 1959, **2**, 129.
32 J. C. Evans, C. C. Rowlands, L. A. Turkson and M. D. Barratt, *J. Chem. Soc., Faraday Trans. 1*, 1988, **84**, 3249.

Paper 0/01418D; *Received* 30*th March*, 1990